Journal of Applied Analysis and Computation
Volume 9, Number 2, April 2019, 615–627
Website:http://jaac.ijournal.cn
DOI:10.11948/2156-907X.20180127

STAGNATION POINT FLOW OF DUSTY CASSON FLUID WITH THERMAL RADIATION AND BUOYANCY EFFECTS

Murugan Muthtamilselvan

Abstract The aim of the study is to examine the stagnation point flow of a dusty Casson fluid over a stretching sheet with thermal radiation and buoyancy effects. The governing boundary layer equations are represented by a system of partial differential equation. After applying suitable similarity transformations, the resulting boundary layer equations are solved numerically using the Runge Kutta Fehlberg fourth-fifth order method (RKF-45 method). The behaviors of velocity, temperature and concentration profiles of fluid and dusty particles with respect to change in fluid particle interaction parameter, Casson paramter, Grashof number, radiation parameter, Prandtl number, number density, thermal equilibrium time, relaxation time, specific heat of fluid and dusty particles, ratio of diffusion coefficients, Schmidt number and Eckert number are analysed graphically and discussed. Our computed results interpret that velocity distribution decays for higher estimation of Casson parameter while temperature distribution shows increasing behavior for larger radiation parameter.

Keywords Casson fluid, dusty fluid, stagnation point, thermal radiation, buoyancy.

MSC(2010) 76D, 76W, 76S.

1. Introduction

Nomenclature

a	Stretching rate
A	Ratio parameter
c_p, c_m	Specific heat capacity of the fluid and dusty particles
C	Concentration of fluid inside boundary layer
C_∞	Ambient fluid concentration
C_p	Concentration of dusty particles at the surface of stretching sheet
$C_{p\infty}$	Ambient particle concentration
C_f	Skin friction coefficient
D	Ratio of diffusion coefficients
D_1, D_2	Diffusion coefficients of fluid and dusty particles respectively
Ec	Eckert number

Email address:muthtamill@yahoo.co.in(M. Muthtamilselvan)
Department of Mathematics, Bharathiar University, Coimbatore-641 046, Tamilnadu, India

g	Acceleration due to gravity
Gr, Gr_c	Thermal Grashof number and Solutal Grashof number
j_w	Mass flux
K	Drag force coefficient (Stoke's resistance)
k^*	Mean absorption coefficient
l	Mass concentration
m	Mass of dusty particle in fluid
N	Number density of particles in dusty phase
Nr	Radiation parameter
Pr	Prandtl number
q_r	Radiative heat flux
q_w	Heat flux
Sc	Schmidt number
Sh	Sherwood number
T	Temperature of the fluid
T_∞	Ambient temperature
T_p	Temperature of dusty phase
(u, v)	Velocity components of the fluid
(u_p, v_p)	Velocity components of the dusty particles
u_e	External flow velocity
u_w	Stretching velocity

Greek Symbols

α	Thermal diffusivity
β	Casson parameter
β^*	Fluid particle parameter
β_T	Volumetric coefficient of thermal expansion
β_C	Volumetric coefficient of thermal expansion with concentration
ρ, ρ_p	Density of fluid and dusty particles
ν	Viscosity of the dusty Casson fluid
σ^*	Stefan-Boltzman constant
τ_T	Thermal equilibrium time
τ_v	Relaxation time of dusty particles
τ_w	Shear stress

The Casson fluid is a shear thining liquid. At zero rate of shear it is assumed to have infinite viscosity, a yield stress below which no flow occurs and a zero viscosity at an infinite rate of shear. Therefore most frequently it functions as a model for depicting steady shear stress as in molten chocolate, blood, tomato sauce, yogurt, concentrated fruit juices, honey, synovial fluids, paints, coal in water, synthetic lubricants and soup. It describes the flow of pigment suspension in preparation of printing inks, suspension of silicon, chocolate and honey. It is also most important in polymer processing and biomechanics industries. A fluid which has immiscible solid particles is known as dusty fluid. The fluids with solid dust particles has significant importance as it is used in purification of crude oil, physiological flows, petroleum processes, dust cloud formed in nuclear explosion, soil preservation, etc. Thermal radiation is most significant in the field of aquifers, power plants for nuclear rockets, hypersonic flights, re-entry space vehicles. Buoyancy is helpful in the research

field of studying underwater waves using research ship called Floating instrument platform (FLIP), the unmanned research vessels used underwater to explore mines, oil and gas, to study the different characteristics of water, in carrying various kinds of fishing nets, acoustic fish finding equipments, sonar and weapon trailling.

Casson fluid behaves like a solid when the yield stress more than shear stress is applied on it. Despite most extreme cases of very high and very low shear rate, the Casson fluid is used as a model because of its accuracy. Casson fluid model involving suspension of particles are widely used in petroleum industries. The stagnation point flow of Casson fluid with homogeneous-heterogeneous reactions is studied by Khan et al. [12]. A mathematical model for the rheological relations of Casson fluid in MHD stagnation point flow is introduced by Khan et al. [13]. A boundary layer flow and heat transfer for a non-Newtonian fluid over a nonlinearly stretching surface is studied by Mukhopadhyay [16]. He found that an increase in Casson parameter enhances the temperature of fluid. Hayat et al. [6] modeled the mixed convection stagnation point flow of an incompressible non-Newtonian Casson fluid over a stretching sheet with convective boundary condition. The MHD stagnation point flow of Casson fluid over a stretched surface with homogeneous-heterogeneous reactions is investigated by Khan et al. [14]. Magnetohydrodynamic flow of Casson fluid over a stretching cylinder is analyzed by Tamoor et al. [24]. They concluded that the velocity and temperature fields enhances away from the cylinder for larger curvature parameter.

Dusty fluid involves the motion of fluids comprising unmixable solid particles. Such examples of dusty fluid systems are flow in rocket tubes, movement of inert solid particles in atmosphere, blood flow in arteries, gas cooling systems in heat transfer process, surface erosion of landing vehicle, etc., Hydromagnetic flow of a dusty fluid over a stretching sheet is studied by Vajravelu and Nayfeh [25]. An unsteady MHD flow and heat transfer of dusty fluid between parallel plates with variable physical properties is analysed by Attia [1]. This model suits many practical applications such as pipes connecting system components, heat exchangers and flow meters. Hossain et al. [7] investigated the unsteady mixed convection dusty fluid flow past a vertical wedge due to small fluctuation in free stream and surface temperature. Numerical solutions for a compressible dusty fluid flow along a vertical wavy cone is derived by Abdullah et al. [2] and it has been discovered that skin friction coefficient decreases as the mass concentration increases and the rate of heat transfer increases when the particles are infused into clear water. The transient MHD couette flow and heat transfer of dusty fluid with variable physical properties is studied by Attia [3].

Flow of an incompressible viscous fluid and heat transfer phenomena over a stretching sheet have received great attention during the past decades owing to the abundance of practical applications in chemical and manufacturing process, such as polymer extrusion, drawing of copper wires, and continuous casting of metals, wire drawing and glass blowing. Flow over a stretching sheet in a dusty fluid with radiation effect is modeled by Ramesh and Gireesha [20]. It can be applied in aerodynamic extrusion of plastic sheets and fibres, drawing, annealing and tinning of copper wire, paper production, crystal growing and glass blowing. These applications involve cooling of a molten liquid and it is necessary that a proper cooling liquid is chosen whose flow is controlled by the stretching sheet. The MHD flow of a dusty fluid near the stagnation point over a permeable stretching sheet with non-uniform source/sink is studied by Ramesh et al. [21]. The heat transfer in

a stagnation point flow towards a stretching sheet is investigated by Mahapatra and Gupta [17]. The stagnation point flow of non-Newtonian fluid towards a nonlinear stretching surface has been considered by many authors, see [8, 9, 15].

The study of heat transfer with thermal radiation has attracted many researchers because of their applications in material dying processes, space technology, hot wiring, solar technology, nuclear plants, production of glass fiber, high temperature processes, heat exchangers, transpiration process, prevention of energy, etc. Bataller [4] analyzed the radiation effects in the blasius flow over a flat plate. The hydromagnetic transport of dust particles in gas flow over an inclined plane with thermal radiation is examined by Mehmood et al. [18]. Enhancement of radiation on hydromagnetic Casson fluid flow towards a stretched cylinder with suspension of liquid-particles is presented by Ramesh et al. [22]. Recently, several investigations have been published about the effect of using radiation in the researches [5, 10, 11, 19, 23].

The present analysis involves the study of stagnation point flow of a dusty Casson fluid that exhibits the phenomenon of thermal radiation and buoyancy during the flow. The steady incompressible flow of dusty Casson fluid is represented by a set of nonlinear partial differential equations which is transformed into a set of ordinary differential equations using similarity transformations. Then the final boundary layer equations are solved using fourth-fifth Runge Kutta Fehlberg method (RKF-45) and examined graphically with respect to various physical parameters.

2. Problem Formulation

Let us consider a two dimensional stagnation flow of dusty Casson fluid over a stretching sheet. The fluid flows as the sheet is stretched along x-axis with velocity $u_w = ax$ where a is the stretching rate. The velocity of fluid in external flow is $u_e = bx$ where b is a positive constant. The origin is being fixed as two equal and opposite forces are applied along x-axis. The stagnation point is being fixed in the path of the fluid flow. The fluid is assumed to be Casson fluid with dusty particles in it. The dusty particles in the fluid are considered to be uniform in size and spherical in shape. The number density of the dusty particles is assumed to be constant throughout the flow of fluid. The buoyancy and thermal radiation effects are considered. A schematic diagram representing the flow is shown in figure 1. The governing boundary layer equations for stagnation point flow of dusty Casson fluid can be written as follows

For the fluid phase

$$\frac{\partial u}{\partial x} + \frac{\partial v}{\partial y} = 0, \tag{2.1}$$

$$u\frac{\partial u}{\partial x} + v\frac{\partial u}{\partial y} = u_e\frac{du_e}{dx} + \nu\left(1+\frac{1}{\beta}\right)\frac{\partial^2 u}{\partial y^2} + \frac{KN}{\rho}\left(u_p - u\right) + g\beta_T\left(T - T_\infty\right) + g\beta_C\left(C - C_\infty\right), \tag{2.2}$$

$$u\frac{\partial T}{\partial x} + v\frac{\partial T}{\partial y} = \alpha\left(\frac{\partial^2 T}{\partial x^2} + \frac{\partial^2 T}{\partial y^2}\right) - \frac{1}{\rho c_p}\frac{\partial q_r}{\partial y} + \frac{N}{\rho\tau_T}\left(T_p - T\right) + \frac{N}{\rho c_p \tau_v}\left(u_p - u\right)^2, \tag{2.3}$$

$$u\frac{\partial C}{\partial x} + v\frac{\partial C}{\partial y} = \frac{\partial}{\partial y}\left(D_1\frac{\partial C}{\partial y}\right). \tag{2.4}$$

For the dusty phase

$$\frac{\partial}{\partial x}(\rho_p u_p) + \frac{\partial}{\partial y}(\rho_p v_p) = 0, \tag{2.5}$$

$$u_p \frac{\partial u_p}{\partial x} + v_p \frac{\partial u_p}{\partial y} = \frac{K}{m}(u - u_p), \tag{2.6}$$

$$u_p \frac{\partial v_p}{\partial x} + v_p \frac{\partial v_p}{\partial y} = \frac{K}{m}(v - v_p), \tag{2.7}$$

$$u_p \frac{\partial T_p}{\partial x} + v_p \frac{\partial T_p}{\partial y} = -\frac{c_p}{c_m \tau_T}(T_p - T), \tag{2.8}$$

$$u_p \frac{\partial C_p}{\partial x} + v_p \frac{\partial C_p}{\partial y} = \frac{\partial}{\partial y}\left(D_2 \frac{\partial C_p}{\partial y}\right), \tag{2.9}$$

with the boundary conditions

$$\begin{gathered} u = u_w = ax,\ v = 0, \\ T = T_w, C = C_w, C_p = C_{pw} \ \text{ at } \ y = 0, \\ u = 0, u_p \to 0, v_p \to v, \\ T \to T_\infty, T_p \to T_\infty, \\ C \to C_\infty, C_p \to C_{p\infty} \text{ as } y \to \infty, \end{gathered} \tag{2.10}$$

$$\tag{2.11}$$

where (u, v) and (u_p, v_p) are the velocity components of the fluid and dusty particles respectively, ν is the coefficient of viscosity of the fluid, β is the Casson parameter, K is the drag force coefficient (Stoke's resistance), N is the number density of the dusty particles in the fluid, m is the mass of the dusty particles in fluid, ρ and ρ_p are the density of fluid and dusty particles in the fluid respectively, g is the acceleration due to gravity, β_T is the thermal expansion coefficient, β_C is the solutal expansion coefficient, T and T_p are the temperature of the fluid phase and dusty phase respectively, C and C_p are the concentration of the fluid phase and dusty phase respectively, α is thermal diffusivity, q_r is the radiative heat flux, c_p is the specific heat capacity of the fluid, c_m is the specific heat capacity of the dusty particles, τ_T is the time required by the dusty particles (thermal equilibrium time) to adjust its temperature to that of fluid, τ_v is the time required by the dusty particles (relaxation time) to adjust its velocity to that of the fluid, D_1 and D_2 are the coefficients of difussion of fluid and dusty particles.

The radiation heat flux q_r can be represented by the use of Rosseland approximation for radiation as

$$q_r = -\frac{4\sigma^*}{3k^*}\frac{\partial T^4}{\partial y}, \tag{2.12}$$

where σ^* is the Stefan-Boltzman constant, k^* is the mean absorption coefficient. Let us consider the differences in temperature of the fluid within the flow can be denoted as a linear function. Therefore T^4 can be expanded in Taylor series. By omitting the higher orders we get,

$$T^4 \cong 4T_\infty^3 T - 3T_\infty^4. \tag{2.13}$$

Substituting (2.13) in (2.12) and differentiating with respect to y, we get

$$\frac{\partial q_r}{\partial y} = -\frac{16\sigma^* T_\infty^3}{3k^*}\left(\frac{\partial^2 T}{\partial y^2}\right). \tag{2.14}$$

The set of partial differential equations representing the flow is converted into system of ordinary differential equations by suitable similarity transformations stated as

$$u = axf'(\eta), v = -\sqrt{a\nu}f(\eta), \eta = \sqrt{\frac{a}{\nu}}y,$$

$$u_p = axF(\eta), v_p = \sqrt{a\nu}G(\eta),$$

$$\theta(\eta) = \frac{T - T_\infty}{T_w - T_\infty}, \theta_p(\eta) = \frac{T_p - T_\infty}{T_w - T_\infty},$$

$$\phi(\eta) = \frac{C - C_\infty}{C_w - C_\infty}, \phi_p(\eta) = \frac{C_p - C_{p\infty}}{C_{pw} - C_{p\infty}}. \tag{2.15}$$

The final boundary layer equations representing the flow system after applying the similarity conditions are as follows

For the fluid phase

$$\left(1+\frac{1}{\beta}\right)f'''(\eta)+f(\eta)f''(\eta)-(f'(\eta))^2+l\beta^*[F(\eta)-f'(\eta)]+Gr\theta(\eta)+Gr_c\phi(\eta)+A^2=0, \tag{2.16}$$

$$(1+Nr)\theta''(\eta)+Prf(\eta)\theta'(\eta)+\frac{PrN}{\rho\tau_T a}[\theta_p(\eta)-\theta(\eta)]+\frac{PrNEc}{\rho\tau_v a}[F(\eta)-f'(\eta)]^2=0, \tag{2.17}$$

$$\phi''(\eta) + Scf(\eta)\phi'(\eta) = 0. \tag{2.18}$$

For the dusty phase

$$F'(\eta)G(\eta) + F^2(\eta) + \beta^*[F(\eta) - f'(\eta)] = 0, \tag{2.19}$$

$$G'(\eta)G(\eta) + \beta^*[f(\eta) + G(\eta)] = 0, \tag{2.20}$$

$$\theta_p'(\eta)G(\eta) + \frac{c_p}{ac_m\tau_T}[\theta_p(\eta) - \theta(\eta)] = 0, \tag{2.21}$$

$$\phi_p''(\eta) - \frac{Sc}{D}\phi_p'(\eta)G(\eta) = 0 \tag{2.22}$$

and the boundary conditions become

$$f'(\eta) = 1, f(\eta) = 0, \theta(\eta) = 1,$$

$$\phi(\eta) = 1, \phi_p(\eta) = 1 \text{ at } \eta = 0, \tag{2.23}$$

$$f'(\eta) = 0, F(\eta) = 0, G(\eta) = -f(\eta), \theta(\eta) = 0,$$

$$\theta_p(\eta) = 0, \phi(\eta) = 0, \phi_p(\eta) = 0 \text{ as } \eta \to \infty, \tag{2.24}$$

where

$Gr = \frac{g\beta_T(T_w - T_\infty)}{a^2x}$ is the thermal Grashof number,

$Gr_C = \frac{g\beta_C(C_{pw} - C_\infty)}{a^2x}$ is the solutal Grashof number,

$Pr = \frac{\nu}{\alpha}$ is Prandtl number,

$Sc = \frac{\nu}{D_1}$ is Schmidt number,

$l = \frac{mN}{\rho}$ is the mass concentration,

$\beta^* = \frac{1}{\tau a}$ is the fluid particle interaction parameter,

$\tau = \frac{m}{K}$ is the relaxation time of the dusty phase,

$D = \frac{D_2}{D_1}$ is the ratio of coeffecients of diffusion,

$Nr = \frac{16\sigma^* T_\infty^3}{3\alpha k^*}$ is the radiation parameter,

$Ec = \frac{a^2 x^2}{c_p(T_w - T_\infty)}$ is the Eckert number.

The surface drag force defined as the force opposing the relative motion of fluid against the stretching sheet is

$$C_f = \frac{\tau_w}{\rho u_w^2}, \tag{2.25}$$

where τ_w is the shear stress given by

$$\tau_w = \left(\mu_B + \frac{p_y}{\sqrt{2\pi_c}}\right)\left(\frac{\partial u}{\partial y}\right)_{y=0}. \tag{2.26}$$

Substituting (2.23) in (2.22)and on solving we get the coefficient of skin friction as

$$C_f Re_x^{1/2} = \left(1 + \frac{1}{\beta}\right) f''(0). \tag{2.27}$$

The local Nusselt number is the rate of heat transfer and can be defined as

$$Nu_x = \frac{x q_w}{k(T_w - T_\infty)}, \tag{2.28}$$

where q_w is the heat flux given as

$$q_w = -k\left(\frac{\partial T}{\partial y}\right)_{y=0}. \tag{2.29}$$

From (2.25) and (2.26),

$$Nu_x Re_x^{-1/2} = -\theta'(0). \tag{2.30}$$

The Sherwood number also known as mass transfer Nusselt number is defined as the rate of mass transfer in the flow and can be represented as

$$Sh_x = \frac{x j_w}{D(C_w - C_\infty)}, \tag{2.31}$$

where j_w is the mass flux denoted as

$$j_w = -D\left(\frac{\partial C}{\partial y}\right)_{y=0}. \tag{2.32}$$

Substitute (2.29) in (2.28) and by solving we get

$$Sh_x Re_x^{-1/2} = -\phi'(0), \tag{2.33}$$

where the Reynolds number $Re_x = \frac{ax^2}{\nu}$.

3. Results and Discussion

The stagnation point flow of a dusty Casson fluid with thermal radiation and buoyancy effects is investigated. The resultant governing equations of the flow (2.16)–(2.22) with the boundary conditions (2.23)–(2.24) are solved numerically and the graphical results on velocity, temperature and concentration profiles for different values of Casson parameter, fluid particle interaction parameter, number density, thermal equilibrium time, relaxation time, specific heat of the fluid and dusty particles, ratio of diffusion coefficients and various physical parameters are studied. The values of the pertinent parameters can be given as $\beta = 0.2$, $l = 0.2$, $\beta^* = 0.5$, $Gr = 2.0$, $Gr_c = 1.0$, $A = 0.1$, $Nr = 1.0$, $Pr = 0.71$, $N = 0.5$, $a = 0.6$, $\rho = 1.0$, $\tau_T = 0.5$, $\tau_v = 1.0$, $Sc = 0.22$, $c_p = 0.2$, $c_m = 0.2$, $D = 1.0$, $Ec = 0.05$ unless stated otherwise.

The velocity profile with respect to the ratio parameter A of the present analysis is compared and a good agreement with the previous study by Khan et al. [12] is obtained in figure 2.

An increase in Casson parameter increases viscosity which opposes the flow of fluid thus decreasing velocity profile shown in figure 3. The decrease of velocity profile in fluid phase and the increase of velocity profile in dusty phase with increase in fluid particle interaction parameter is depicted in figure 4. The effect of thermal Grashof number on velocity, temperature and concentration profiles is revealed in figures 5–7. An increase in thermal Grashof number increases the velocity profile, decreases the temperature and concentration profiles in both fluid and dusty phase. figures 8–10 represent the variation of velocity, temperature and concentration with the respect to solutal Grashof number. As the solutal Grashof number increases, the velocity profile increases and the temperature and concentration profiles decreases in both fluid and dusty phase. Due to the decrease in Rosseland radiative absorptivity, an increase in rate of radiative heat transfer of the fluid is noticed which makes the fluid temperature to increase as illustrated in figure 11.

Since Prandtl number is the ratio of kinematic viscosity and thermal diffusivity, small value Pr fluids show high rate of thermal diffusivity thus increasing temperature distribution as evidenced in figure 12. The thermal boundary layer decreases with an increase in number density in both fluid and dusty phase is seen in figure 13. In figure 14, an increase in thermal equilibrium time decreases the temperature distribution in dusty phase and increases the thermal boundary layer in fluid phase. Higher value of relaxation time of dusty particles exhibit non-conductivity of the fluid which decreases the temperature distribution as in figure 15. The thermal boundary layer increases with an increase in specific heat of the fluid and decreases with an increase in specific heat of the dusty particles as shown in figure 16 and figure 17 respectively.

Figure 18 depicts that an increase in ratio of diffusion coefficients increases concentration profile in dusty phase whereas there is no change in fluid phase. The flow of fluid in which different mass and momentum diffusion processes involved can be described easily with the help of Schmidt number. Higher value of Schmidt number decreases mass diffusion rate which makes the particles to divert away and thus decaying the concentration boundary layer in both phases as illustrated in figure 19. When Eckert number is high, the fluid particles are more energetic because of energy storage and hence the thermal boundary layer increases in both fluid and dusty phase as represented in figure 20.

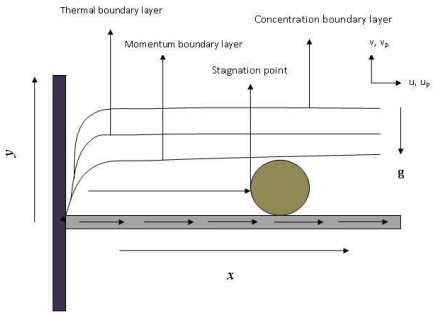

Figure 1. Schematic diagram of the stagnation point flow of dusty Casson fluid

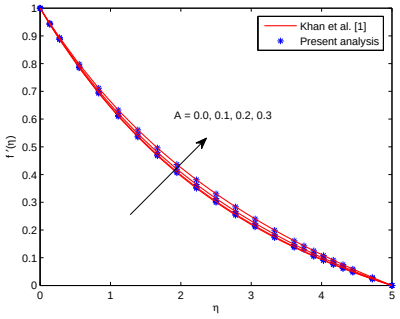

Figure 2. Comparison of velocity profile

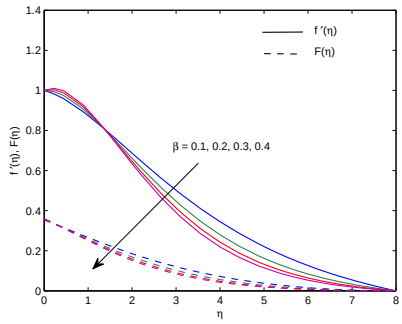

Figure 3. Effect of Casson parameter on velocity profile

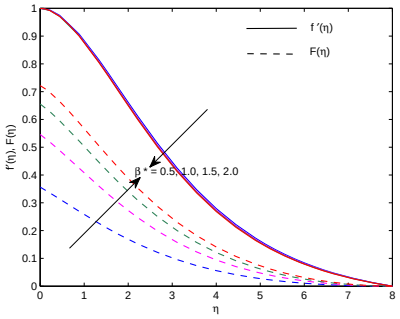

Figure 4. Effect of fluid particle interaction parameter on velocity profile

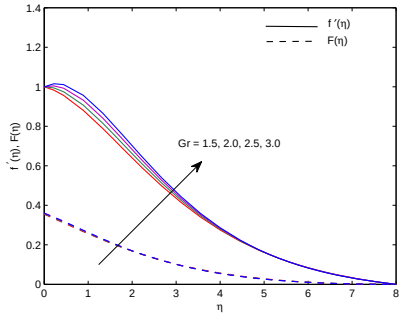

Figure 5. Effect of thermal Grashof number on velocity profile

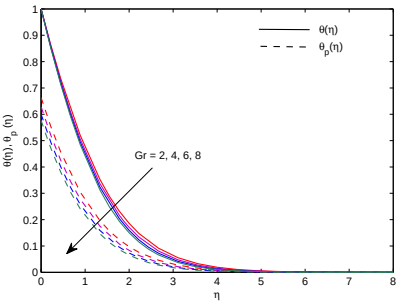

Figure 6. Effect of thermal Grashof number on temperature profile

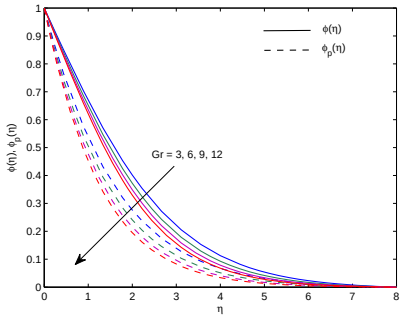

Figure 7. Effect of thermal Grashof number on concentration profile

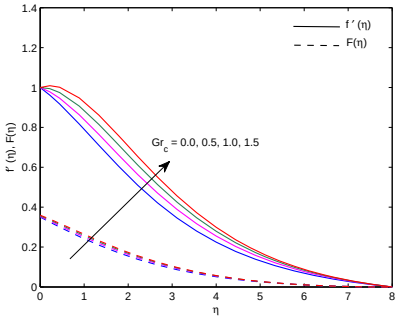

Figure 8. Effect of solutal Grashof number on velocity profile

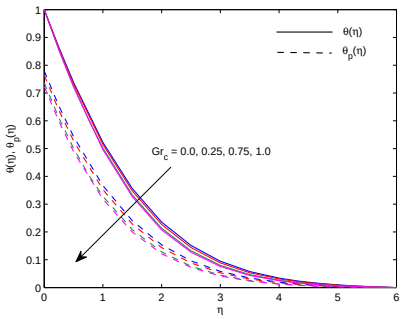

Figure 9. Effect of solutal Grashof number on temperature profile

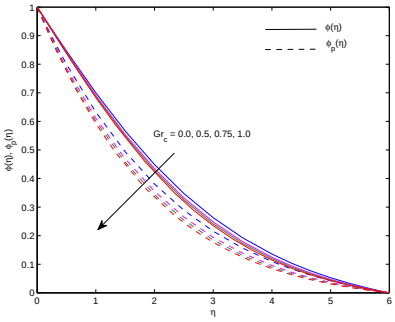

Figure 10. Effect of solutal Grashof number on concentration profile

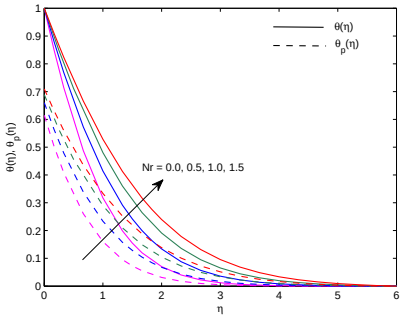

Figure 11. Effect of radiation parameter on temperature profile

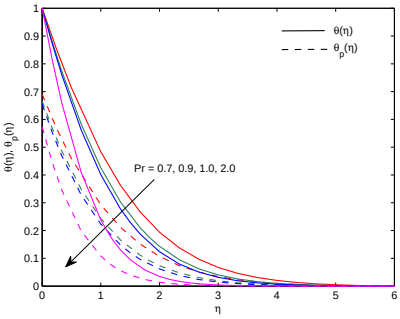

Figure 12. Effect of Prandtl number on temperature profile

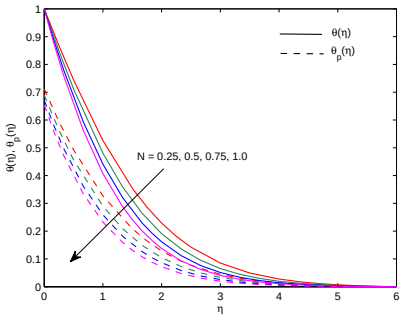

Figure 13. Effect of number density parameter on temperature profile

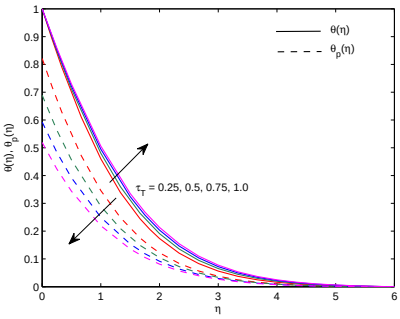

Figure 14. Effect of thermal equilibrium time on temperature profile

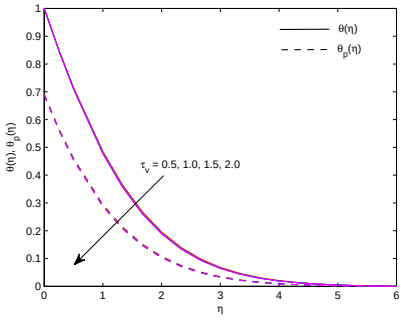

Figure 15. Effect of relaxation time on temperature profile

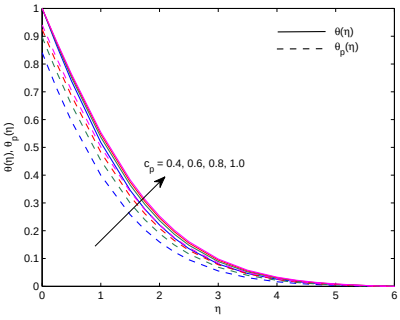

Figure 16. Effect of specific heat of fluid on temperature profile

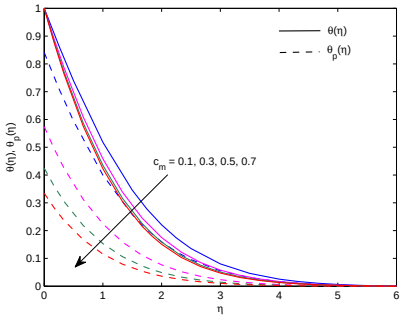

Figure 17. Effect of specific heat of dusty particles on temperature profile

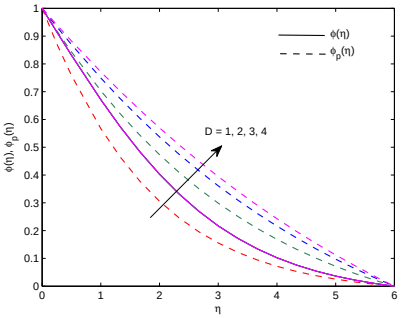

Figure 18. Effect of ratio of diffusion coefficients on concentration profile

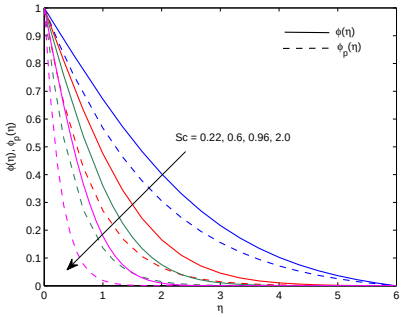

Figure 19. Effect of Schmidt number on concentration profile

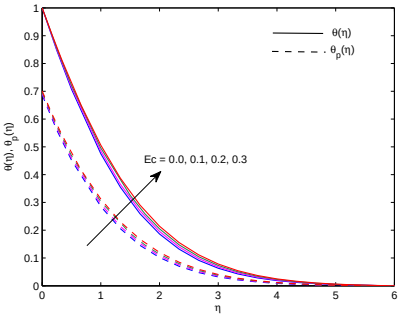

Figure 20. Effect of Eckert number on temperature profile

4. Conclusion

The stagnation point flow of dusty Casson fluid over a stretching sheet has been analyzed. The governing boundary layer equations are reduced to a set of ordinary differential equation with the help of appropriate similarity transformations. Then the RKF-45 method is used to solve the final transformed equations numerically. The graphical interpretation of the impact of various physical parameters on velocity, temperature and concentration profiles in both fluid and dusty phase are presented. The main results of the analysis are as follows:

- The variation in Casson parameter decelerates the velocity in both fluid and dusty phase as there is an increase in viscosity of the fluid. In fluid and dusty phase, both thermal and solutal Grashof number increases the momentum boundary layer and decreases the thermal and concentration boundary layers.
- The effect of radiation parameter increases the temperature of the fluid. Therefore radiation must be kept at minimum to avoid the temperature rise in fluid flow. The thermal boundary layer decays with increase in Prandtl number, number density, relaxation time in both fluid and dusty phase. For different values of thermal equilibrium time, the temperature increases in fluid phase and decreases in dusty phase.
- Temperature distribution increases with increase in specific heat of the fluid and decreases with increase in specific heat of dusty particles. In fluid phase

increase of ratio of diffusion coefficients shows no effect on concentration profile whereas the concentration profile increases in dusty phase.

- Larger Schimdt number decreases the concentration distribution because of reduced diffusion rate in both phases. As the Eckert number increases, the thermal boundary layer enlarges in both fluid and dusty phase.

Acknowledgements. The authors are grateful to the anonymous referees for their useful suggestions which improve the contents of this article.

References

[1] H. A. Attia, *Unsteady MHD flow and heat transfer of dusty fluid between parallel plates with variable physical properties*, Applied Mathematical Modelling, 26(2002), 863–875.

[2] A. Abdullah, A. Rashed, S. Siddiqa, N. Begum and Md. A. Hossain, *Numerical solutions for a compressible dusty fluid flow along a vertical wavy cone*, International Journal of Heat and Mass Transfer, 108(2017), 1229–1236.

[3] H. A. Attia, *Unsteady MHD Couette flow and heat transfer of dusty fluid with variable physical properties*, Applied Mathematics and Computation, 177(2006), 308–318.

[4] R. C. Bataller, *Radiation effects in the blasius flow*, Applied Mathematics and Computation, 198(2008), 333–338.

[5] D. H. Doh, M. Muthtamilselvan, E. Ramya and P. Revathi, *Effects of thermal radiation on a 3D sisko fluid over a porous medium using Cattaneo-Christov heat flux model*, Communications in Theoretical Physics, 70(2018), 230–238.

[6] T. Hayat, S. A. Shehzad, A. Alsaedi and M. S. Alhothuali, *Mixed convection stagnation point flow of Casson fluid with convective boundary conditions*, Chinese Physics Letters, 29(2012), 1147041-1147044.

[7] Md. A. Hossain, N. C. Roy and S. Siddiqa, *Unsteady mixed convection dusty fluid flow past a vertical wedge due to small fluctuation in free stream and surface temperature*, Applied Mathematics and Computation, 293(2017), 480–492.

[8] T. Hayat, M. Ijaz Khan, M. Farooq, A. Alsaedi, M. Waqas and T. Yasmeen, *Impact of Cattaneo-Christov heat flux model in flow of variable thermal conductivity fluid over a variable thicked surface*, International Journal of Heat and Mass Transfer, 99(2016), 702–710.

[9] T. Hayat, M. Ijaz Khan, M. Farooq and A. Alsaedi, *Stagnation point flow with Cattaneo-Christov heat flux and homogeneous-heterogeneous reactions*, Journal of Molecular Liquids, 220(2016), 49–55.

[10] T. Hayat, M. Ijaz Khan, M. Waqas, A. Alsaedi and M. Imran Khan, *Radiative flow of micropolar nanofluid accounting thermophoresis and Brownian moment*, International Journal of Hydrogen Energy, 42(2017), 16821–16833.

[11] T. Hayat, S. Qayyum, M. Khan and A. Alsaedi, *Entropy generation in magnetohydrodynamic radiative flow due to rotating disk in presence of viscous dissipation and Joule heating*, Physics of Fluids, 30(2018), 017101.

[12] M. I. Khan, M. Waqas, T. Hayat and A. Alsaedi, *A comparative study of Casson fluid with homogeneous-heterogeneous reactions*, Journal of Colloid and Interface Science, 498(2017), 85–90.

[13] M. I. Khan, T. Hayat, M. I. Khan and A. Alsaedi, *A modified homogeneous-heterogeneous reactions for MHD stagnation point flow with viscous dissipation and joule heating*, International Journal of Heat and Mass Transfer, 113(2017), 310–317.

[14] M. I. Khan, M. Waqas, T. Hayat and A. Alsaedi, *Magnetohydrodynamic (MHD) stagnation point flow of Casson fluid over a stretched surface with homogeneous-heterogeneous reactions*, Journal of Theoretical and Computational Chemistry, 16(2017), 175002201-175002213.

[15] M. Ijaz Khan, M. Waqas, T. Hayat and A. Alsaedi, *A comparative study of Casson fluid with homogeneous-heterogeneous reactions*, Journal of Colloid and Interface Science, 498(2017), 85–90.

[16] S. Mukhopadhyay, *Casson fluid flow and heat transfer over a nonlinearly stretching surface*, Chinese Physics B, 22(2013), 0747011-0747015.

[17] T. R. Mahapatra and A. S. Gupta, *Heat transfer in stagnation point flow towards a stretching sheet*, Heat and Mass Transfer, 38(2002), 517–521.

[18] O. U. Mehmood, M. M. Maskeen and A. Zeeshan, *Hydromagnetic transport of dust particles in gas flow over an inclined plane with thermal radiation*, Results in Physics, 2017(2017), 1–16.

[19] M. Muthtamilselvan and S. Sureshkumar, *Convective heat transfer in a nanofluid-saturated porous cavity with the effects of various aspect ratios and thermal radiation*, Physics and Chemistry of Liquids, 55(2018), 617–636.

[20] G. K. Ramesh and B. J. Gireesha, *Flow over a stretching sheet in a dusty fluid with radiation effect*, Journal of Heat Transfer, 135(2013), 1027021-1027026.

[21] G. K. Ramesh, B. J. Gireesha and C. S. Bagewadi, *MHD flow of a dusty fluid near the stagnation point over a permeable stretching sheet with non-uniform source/sink*, International Journal of Heat and Mass Transfer, 55(2012), 4900–4907.

[22] G. K. Ramesh, K. G. Kumar, S. A. Shehzad and B. J. Gireesha, *Enhancement of radiation on hydromagnetic Casson fluid flow towards a stretched cylinder with suspension of liquid-particles*, Canadian Journal of Physics, 96(2018), 18–24.

[23] E. Ramya, M. Muthtamilselvan and D. H. Doh, *Absorbing/emitting radiation and slanted hydromagnetic effects on micropolar liquid containing gyrostatic microorganisms*, Applied Mathematics and Computation, 324(2018), 69–81.

[24] M. Tamoor, M. Waqas, M. I. Khan, A. Alsaedi and T. Hayat, *Magnetohydrodynamic flow of Casson fluid over a stretching cylinder*, Results in Physics, 7(2017), 498–502.

[25] K. Vajravelu and J. Nayfeh, *Hydromagnetic flow of a dusty fluid over a stretching sheet*, International Journal of Non-Linear Mechanics, 27(1992), 937–945.